

The Dynamics of Group Flights of an Unmanned Aerial Vehicle

Lucjan Setlak and Rafał Kowalik

Aviation Division, Department of Avionics and Control Systems

Polish Air Force University

Deblin 08-521, ul. Dywizjonu 303 No. 35

Poland

l.setlak@law.mil.pl, r.kowalik@law.mil.pl

Abstract: - The subject of this article is to present the issue of coordination of various formations of unmanned aerial vehicles, which currently play an important role in modern aviation both in the aspect of performing military and civil tasks. Issues of this kind attracted a lot of attention, among others due to achieving potential benefits, which include various types of issues reflected in practical applications in the form of: supervision, exploration of natural resources, atmosphere research, or the implementation of tasks from the military (search, rescue, reconnaissance and destruction of targets in a large area). The main goal of the article is to investigate the dynamics of UAV objects moving in a group flight by conducting a critical analysis of the subject literature, developing a model of prediction method for flight formation of UAV objects and on this basis performing simulation tests in the Matlab/Simulink programming environment. The final part of the article presents the results obtained from the simulation tests for the considered cases of flight of UAV objects, on the basis of which practical conclusions were formulated.

Key-Words: - Dynamic analysis, group flights, unmanned aerial vehicle

1 Introduction

As the unmanned aerial vehicles develop, interesting views appear about their possible applications. Currently, unmanned aerial vehicles are used for various types of military and civil tasks. In order to increase the efficiency of tasks performed by UAV objects, they began to apply them to group flights.

A group flight is defined as a flight of aircraft with certain positions relative to each other, carried out by the group commander. In turn, the flight in the formation is the intended movement of two or more flying objects, which are connected by a common control system, in order to achieve and maintain a specific shape of the whole formation, maintaining appropriate speeds and distances through individual members and avoiding collisions between objects [1], [2].

The most frequently mentioned advantage of a group flight is its use in terrain searching. Each of the objects has a specific range of space monitoring, and in exploration missions it is important to move and comb the entire area as quickly as possible.

By giving the proper shape of the formation and the placement of objects in the group, whose observation and measurement devices will be in contact, it is possible to carry out the task in the best possible way.

In order to solve the problem of controlling a group of UAV objects, it is first of all necessary to ensure an appropriate degree of autonomy and stability for each member of the group. Each of the flying objects must be able to achieve and monitor the set speed, direction and altitude, while the stability of the position of one object will determine the stability of the whole group of UAV objects.

The article presents the problem of controlling the group flight of UAV objects. In this respect, the flight stability of a pair of flying objects in the formation was analyzed, considering three cases, namely: taking into account constraints in the controller's formula, avoiding collisions with large obstacles and avoiding collisions with small or unremembered obstacles.

Moreover, in the further part of the work, selected simulation tests were carried out in the Matlab/Simulink program in terms of the analysis of 6 flight cases of the formation of flying objects.

2 Model of the predictive control method for formation flight

Currently, the problem of flight in the formation of many unmanned aerial vehicles is primarily the achievement of formation and the implementation of joint maneuvers in this formation. Mainly, UAV

objects are individually targeted. The purpose of this subsection is to develop a model designed to control the formation of many unmanned aerial vehicles.

It is still an open and demanding problem, especially in the scope of taking into account such factors as: communication between unmanned aerial vehicles, external influence of the environment in the form of e.g. wind, or non-linear dynamics of unmanned aircrafts. The main goal of the proposed solution is to achieve the individual dynamics of the flying apparatus and to provide data during maneuvering in real time while avoiding collisions with various types of obstacles [3], [4].

In the predictive model (prediction) of the flight path of a potential UAV, the current flight control is provided via a wireless link. The system calculates the optimal control sequence, as a result, the first command in the sequence is passed to the flying object before the next refresh of the transmitted information.

It was assumed that there are "m" UAVs in formation in such a way that at each step only one set of control inputs of the updated unmanned aircraft can be set. After updating the "m" UAV objects, a new update cycle is started so that each entire cycle repeats after the cycle time T .

It should be noted that this type of model is used to control flying objects, which are characterized by a sufficiently low flight dynamics in order to ensure sufficient data refreshing rate between sent commands. As a result, along with the development of faster and more powerful computers, it will be possible to introduce this model to more dynamic and faster flying objects.

2.1 Formation kinematics

For the purpose of linking in the scope of the functions of the lead persons, i.e. a leader (*leader aircraft*) and a wingman (*wingman aircraft*) of the unmanned aerial vehicle, spatial coordinates and rotational coordinates related to the Earth and the UAV wingman object were used.

For the purpose of establishing a coordinate rotary wing-like flying apparatus, the axis stabilization system is used in this way that the axis x^B is chosen for this purpose so that it can cover with a wingspan vector V_w , with the axis Y^B aligned in a straight line with the direction of the UAV wing object, and axis Z^B is complementing the right-hand *Cartesian* coordinate system [5], [6].

In order to present the definition of spatial coordinate, the axis X^S is chosen in order to indicate the north, the axis Y^S is directed to the east, while the axis Z^S completes the clockwise *Cartesian* coordinate system.

These two coordinate systems configured in the above manner are illustrated in the figure below (Fig. 1).

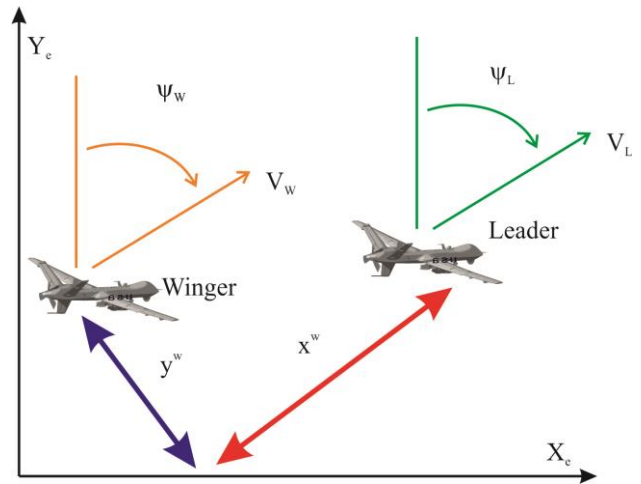


Fig. 1. Coordinates relating to the flight of the UAV formation

As a result of the considerations in the aspect of lead (*lead*)-wing (*wing*) separation, kinematic equations were obtained, referring to the rotary coordinate attached to the wing of the UAV object.

In turn, using the law of speed transformation, the following equations (1) - (7) were obtained:

$$V_L^B = V_{WL}^B + V_W^B + \omega_W^B \cdot R_{WL}^B \quad (1)$$

where:

V_L^B - is the speed of inertia of the leader UAV object in the rotating reference frame;

V_{WL}^B - determines the speed of the leader aircraft with respect to the wing expressed in the rotating reference frame;

V_W^B - is the speed of the UAV wing object in the rotating reference frame;

ω_W^B - means the angular speed of the UAV wing object in the rotating reference frame;

R_{WL}^B - defines the position of the leading UAV object with respect to the wing in the rotating reference frame.

Remarks:

$$V_W^B = \begin{bmatrix} V_W \\ 0 \\ 0 \end{bmatrix}, \quad \omega_W^B = \begin{bmatrix} 0 \\ 0 \\ \psi_W \end{bmatrix}, \quad R_{WL}^B = \begin{bmatrix} x^B \\ y^B \\ z^B \end{bmatrix} \quad (2)$$

where:

$$\psi_e = \psi_L - \psi_W$$

therefore, from the above equations was obtained:

$$V_{WL}^B = \begin{bmatrix} V_L \cos \psi_e \\ V_L \sin \psi_e \\ 0 \end{bmatrix} - \begin{bmatrix} -\dot{\psi}_w y^B \\ \dot{\psi}_w x^B \\ 0 \end{bmatrix} - \begin{bmatrix} V_W \\ 0 \\ 0 \end{bmatrix} \quad (3)$$

At the same time, the components V_{WL}^B can be expressed as:

$$V_{WL}^B = i \cdot \dot{x}^B + j \cdot \dot{y}^B + k \cdot \dot{z}^B \quad (4)$$

so:

$$\dot{x}^B = V_L \cos \psi_e + \dot{\psi}_w y^B - V_W \quad (5)$$

$$\dot{y}^B = V_L \sin \psi_e - \dot{\psi}_w x^B \quad (6)$$

$$\dot{z}^B = 0 \quad (7)$$

The above equations describe the kinematics of formation, which will be used to develop the law of formation control. The purpose of the control is to control the equilibrium states (specific shapes of the formation).

It should be noted that although UAV objects will be separated, their dynamics will be coupled due to the creation requirement. The rest of the unmanned aerial vehicles as adjacent were attached to each unmanned aerial vehicle.

In this arrangement, the unmanned aerial vehicles cooperate with each other. The closely related dynamics of each of them affects the impact on the movement of the other unmanned aerial vehicles [7], [8].

The definition of formation of a UAV object can be given as a combined formation kinematics, i.e. equations (5) - (7) and automatic pilots:

$$\dot{V} = -\frac{1}{\tau_v} (V - V_C) \quad (8)$$

$$\dot{\psi} = -\frac{1}{\tau_\psi} (\psi - \psi_C) \quad (9)$$

where: τ_ψ and τ_v - are constants of the time of the automatic pilot responding.

In the next stage of the analysis, the process of linearization of equations around the nominal point of flight of the formation was made ($[\bar{x}, \bar{V}_w, \bar{V}_L, \bar{y}, \bar{\psi}_w, \bar{\psi}_L]^T$), as a result of which the leading-tracking equation was obtained in the following form (10), (11):

$$\dot{x} = A_c x + B_c u \quad (10)$$

$$y = C_c x \quad (11)$$

where:

A_c, B_c and C_c - are matrix coefficients.

$$A_c = \begin{bmatrix} 0 & -1 & 1 & 0 & -\frac{\bar{y}}{\tau_\psi} & 0 \\ 0 & \frac{-1}{\tau_v} & 0 & 0 & 0 & 0 \\ 0 & 0 & \frac{-1}{\tau_v} & 0 & 0 & 0 \\ 0 & 0 & 0 & 0 & \left(\frac{\bar{x}}{\tau_\psi} - \bar{V}\right) & \bar{V} \\ 0 & 0 & 0 & 0 & \frac{-1}{\tau_\psi} & 0 \\ 0 & 0 & 0 & 0 & 0 & \frac{-1}{\tau_\psi} \end{bmatrix} \quad (12)$$

$$B_c = \begin{bmatrix} 0 & \frac{\bar{y}}{\tau_\psi} \\ \frac{1}{\tau_v} & 0 \\ 0 & 0 \\ 0 & \frac{\bar{x}}{\tau_\psi} \\ 0 & \frac{1}{\tau_\psi} \\ 0 & 0 \end{bmatrix} \quad (13)$$

$$C_c = \begin{bmatrix} 1 & 0 & 0 & 0 & 0 & 0 \\ 0 & 1 & -1 & 0 & 0 & 0 \\ 0 & 0 & 0 & 1 & 0 & 0 \\ 0 & 0 & 0 & 0 & 1 & -1 \end{bmatrix} \quad (14)$$

where: \bar{y}, \bar{x} and \bar{v} - mean the nominal value of a formation flight.

The state vector is equal to:

$x = [x, V_w, V_L, y, \psi_w, \psi_L]^T$, and the input vector is: $u = [V_{wc}, \psi_{wc}]^T$, where the first two are manipulated variables, while the last two are measured disturbances.

The output vector is:

$$y = [x, V_L - V_W, y, \psi_L - \psi_W]^T.$$

Using the "c2d" function in the MATLAB program, we can download a continuous model in the discrete form shown below (15), (16):

$$x(k+1) = A_1 x(k) + B_1 u_1(k) \quad (15)$$

$$y(k) = C_1 x(k) \quad (16)$$

In turn, due to the fact that the predictive control algorithm will actually generate changes instead of u , it will be possible for many purposes to perceive the "controller" as signal generation Δu , and "model" as this input signal [9], [10].

One way to change the input signal to Δu is to define a state vector:

$$\xi(k) = \begin{bmatrix} \Delta x(k) \\ y(k-1) \end{bmatrix} \quad (17)$$

Then the extended nominal model can be written in the form (18), (19):

$$\xi(k+1) = A\xi(k) + B\Delta u(k) \quad (18)$$

$$y(k) = Cx(k) \quad (19)$$

where:

$$A = \begin{bmatrix} A_1 & 0 \\ C_1 & I \end{bmatrix}, B = \begin{bmatrix} B_1 \\ 0 \end{bmatrix}, C = (C_1 I)$$

It can be shown that predictions based on the extended state model are equal (20):

$$\begin{bmatrix} \hat{y}(k+1) \\ \hat{y}(k+2) \\ \vdots \\ \hat{y}(k+N) \end{bmatrix} = \begin{bmatrix} CA \\ CA^2 \\ \vdots \\ CA^N \end{bmatrix} \xi(k) + \begin{bmatrix} CB & 0 & \dots & 0 \\ CAB & CB & 0 & \vdots \\ \vdots & \vdots & \ddots & \vdots \\ CA^{N-1}B & \dots & \dots & CB \end{bmatrix} \begin{bmatrix} \Delta \hat{u}(k|k) \\ \Delta \hat{u}(k+1|k) \\ \vdots \\ \Delta \hat{u}(k+N-1|k) \end{bmatrix} \quad (20)$$

or in vector notation (21):

$$\hat{Y} = \Phi \xi(k) + G \hat{U} \quad (21)$$

The formation flight control algorithm can be described in the following way:

- obtaining the current model of the output signal $y(k)$;
- calculation of the required input signal model $\Delta u(k)$ and respecting entry and exit constraints;
- application $\Delta u(k)$ in the model.

The full structure of the system is illustrated in the figure above (Fig. 2). In a formation flight, each UAV wingman is equipped with one controller to maintain certain distances from the leader, where the formation leader is commanded by a ground control station GCS (*Ground Control System*).

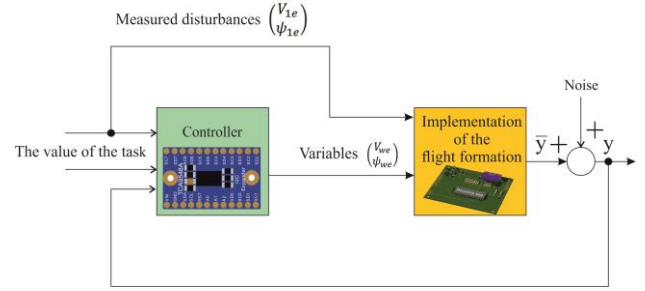


Fig. 2. Diagram of flight and signal formation

2.2 A pair stability of unmanned UAV objects in formation

System stability is well defined for various limitations and gain functions for linear and non-linear systems. This subsection uses terminal restrictions to ensure the stability of the formation flight system.

2.2.1 Taking into account constraints in the controller formula

As mentioned below, the control method can directly meet the constraints. This section presents a simulation of a fast course change of 60 degrees, which has the ability to cope with the controller's constraints during the flight of the formation of UAV objects [11], [12].

The simulation used a model of a UAV object with fixed wings, where the time constants of the automatic pilot of the UAV object were respectively: $\tau_v = 5$ [s] and $\tau_\psi = 0.75$ [s].

In the controller, the horizon of the predictive control N_u and the predictive horizon N_2 are set as $N_u = 3$ and $N_2 = 20$, where the test time is 0.2 [s].

The control signal is limited and the output limits are set as (22) - (25):

$$\Delta V_{min} \leq \Delta V_c \leq \Delta V_{max} \quad (22)$$

$$\Delta \psi_{min} \leq \Delta \psi_c \leq \Delta \psi_{max} \quad (23)$$

$$x_{min} \leq x \quad (24)$$

$$y_{min} \leq y \quad (25)$$

The limits are selected as (26) - (31):

$$\Delta V_{min} = -0.2 \left(\frac{m}{s} \text{ a step} \right) \quad (26)$$

$$\Delta V_{max} = 0.2 \left(\frac{m}{s} \text{ a step} \right) \quad (27)$$

$$\Delta \psi_{min} = -0.07 \left(\frac{rad}{step} \right) \quad (28)$$

$$\Delta\psi_{max} = 0.07\left(\frac{rad}{step}\right) \quad (29)$$

$$x_{min} = 1 [m] \quad (30)$$

$$y_{min} = 1 [m] \quad (31)$$

The nominal desired separation is: $\bar{x} = 2 [m]$, $\bar{y} = 2 [m]$, where the flight speed of a pair of UAV objects in the formation is $2 \frac{m}{s}$, whereby the leader immediately rotates by an angle of 60 degrees. In this simulation, in order to check whether the controller copes with constraints, it is assumed that the leader does not have the same limitations.

The reaction of the UAV wing object is presented in the next figure (Fig. 3), and the control inputs, i.e. the input data of the set speed and the course angle input data for the UAV object, are shown in the following figures (Figs. 4-5). Based on the analysis of Fig. 6, it can be observed that after about 0.2 [s] and 7 [s] the change of the speed control input signal is large, because the UAV object tries to maintain the pattern, but because of the limitation of the input speed change never exceeds $0.2 \frac{m}{s}$ a step (performed action) [13], [14].

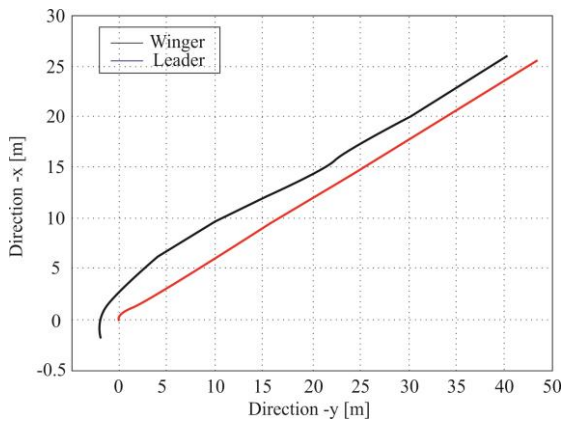


Fig. 3. Graph of separation between the leader and the wing UAV object

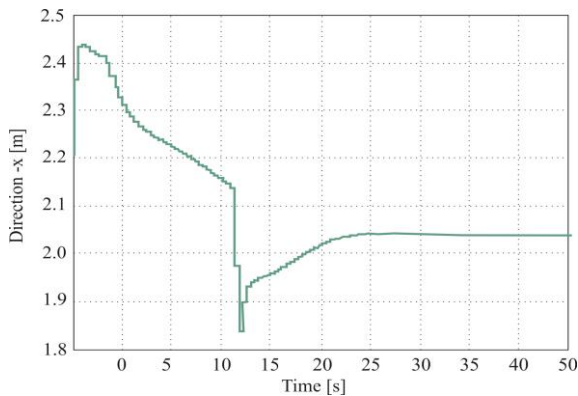


Fig. 4. Graph of the speed control input

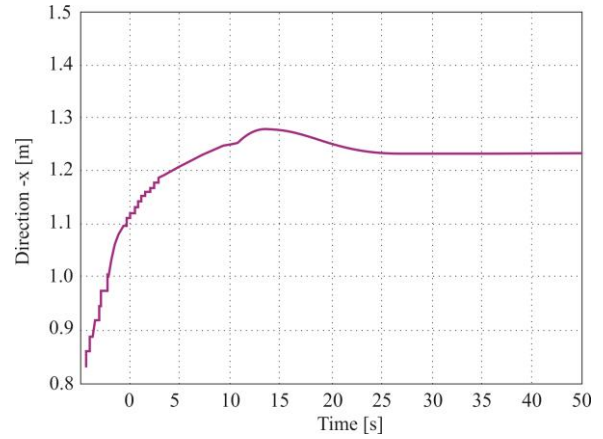


Fig. 5. Graph of the direction control input

From the simulation above, it can be deduced that the controller's approach in this case may work correctly. This sub-chapter analyzes the theories concerning the controller. Next, a generalized, limited formula of the controller in flight of the UAV object formation was discussed. The results presented here essentially guarantee only nominal stability, because the lack of uncertainty or distortion are treated as part of the problem. The simulation results are also presented.

2.2.2 Avoiding collisions with large obstacles

Multi-top (multi-cell) is used to illustrate various types of obstacle shapes. To this end, to ensure that each trajectory point of the UAV object is not within the boundaries of the given obstacle, the binary variables are entered in the formula of restriction.

For example, when considering an obstacle in the shape of a hexagon, each edge can be considered a hyperplane, which divides the flying zone into two halves of this space, one being safe and the other not.

In the formulation of collision avoidance constraints, the predicted future point on the trajectory of the flight of each UAV object is connected to the table of binary variables [15], [16].

In the case of an obstacle in the shape of a hexagon, a set of 6 binary variables is attached to each predicted point.

The mathematical record takes the following form (32), (33):

$$b_i = 1 \text{ if } x \in \{x | a_i^T x < b_i\} \quad (32)$$

$$\sum_{i=1}^6 b_i \geq 1 \quad (33)$$

where: b - is a binary table of variables attached to the predicted position x .

For every edge the hyperplane can be defined $\{x|a_i^T x = b_i\}$, where $\{x|a_i^T x < b_i\}$ - means a safe space for a potential UAV object.

The above wording means that the expected point should be in a safe half-space. In addition, it should be noted that more edges correspond to a larger number of binary variables in the formulation, and therefore more time will be needed in the optimization calculations [17], [18].

In turn, if this is a problem, a reduced representation of the shape can be used. For example, a hexagon can be used to represent a circular obstacle.

2.2.3 Avoiding collisions of small or unremembered obstacles

In this part, the shape of a small obstacle is referred to as a circle or cylinder, but it should be noted that if the shape of an obstacle is not a circle or cylinder, then the collision avoidance algorithm can still be used after some modifications.

In the proposed approach, position restrictions are calculated using the points of intersection of the spatial horizon of the aircraft H_i and obstacle.

Assuming that the range of the obstacle detection sensor H_i is greater than the distance that the UAV object is able to defeat in one step, then any unknown obstacles within the range H_i will be successfully detected, as illustrated in the figure below (Fig. 6).

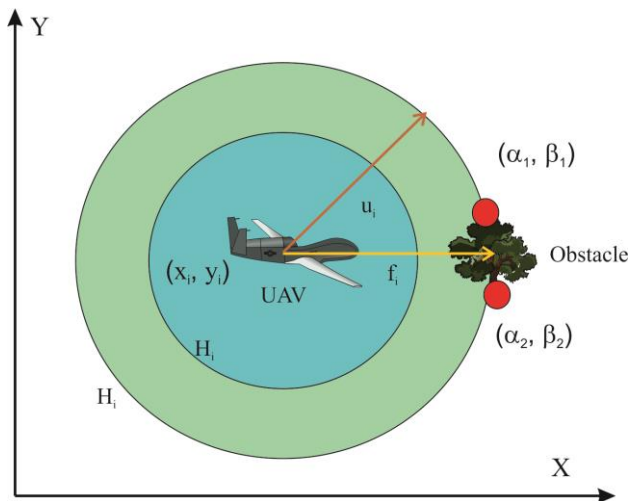


Fig. 6. Avoiding a collision with a small obstacle

A temporary smaller spatial horizon of the UAV object can be set H_{i*} , based on the distance between it and the obstacle and points of intersection with an obstacle.

A constraint to the controller formula can be added to deal with this type of scenario (34):

$$norm(\hat{x}_{k+1} - x_k) \leq H_{i*} \quad (34)$$

where: \hat{x}_{k+1} and x_k - denote respectively the next predicted position and the current position.

It should be noted that this position limitation does in fact make it impossible to position the next vehicle predictive position out of H_i , which ensures that the UAV object will not pass through the obstacle, and this limitation does not negatively affect optimization [19], [20]. The illustration of the entire collision avoidance pattern is shown in the next figure (Fig. 7).

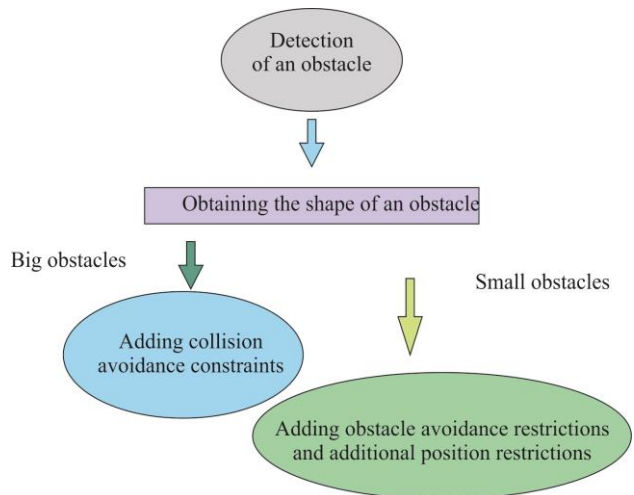


Fig. 7. Diagram of collision avoidance by the UAV object

3 Results of simulation tests

This chapter presents some of the simulation results of a decentralized control scheme composed of multiple events without a collision.

The model of the UAV object used in the simulations is a small quadcopter with the controller installed.

Most of the simulations are performed in 2D space, however, it can be easily expanded to three-dimensional 3D space.

The 2D representation has been chosen because it facilitates the visualization of the trajectory of the object in a clearer way.

The connection is described by means of a graph, which is drawn from the two nearest neighbors visible for each UAV object [21].

It is important that the proposed method in this chapter can easily include any other specific UAV object dynamics described by higher accuracy, heterogeneity, more complex linear or semi-linear models.

Details of the simulation configuration are discussed below, namely:

1. Predictive horizon N_u as $N_u = 3$. Let's assume that the simulations do not have a delay, and the sample time is set to 0.3 [s].

In a multiplexed, reliable, decentralized scheme, the update interval between subsystems of the UAV object is 0.1 [s].

2. The following simulations are performed using a multiplexed, decentralized scheme, and the update cycle is sequential, i.e. (1, 2, 3, 1, 2, 3 ...), except that in case of the 5 update cycle it is (1, 2, 1, 3, 1, 2, 1, 3, ...).
3. Taking into account the system dynamics and the principle of interconnection "two nearest neighboring UAV objects", each UAV object solves a decentralized optimization problem with a profit function.
4. Each UAV object in the formation has identical dynamics.
5. The linear speed limits of a single object are equal (35):

$$\begin{aligned} |v| \\ \leq [V_{xmax} V_{ymax} V_{zmax}]^T \\ = [555]^T [m] \end{aligned} \quad (35)$$

1. Connection restrictions (collision avoidance) are represented by (36):

$$\begin{aligned} q^{i,j}(x_k^i, u_k^i, x_k^j, u_k^j) \\ = d_{sec.} \\ - \|y_{k,pos}^i - y_{k,pos}^j\|_{inf} \\ \leq 0, d_{sec.} = \\ = 0.5 [m] \end{aligned} \quad (36)$$

2. Limitations of network connectivity:

$$\begin{aligned} q^{i,j}(x_k^i, u_k^i, x_k^j, u_k^j) \\ = \|y_{k,pos}^i - y_{k,pos}^j\|_{inf} \\ - d_{com} \leq 0, d_{sec.} = \\ = 10 [m] \end{aligned} \quad (37)$$

The values in the function of costs are selected as: $Q_f = I$ for all UAV objects, where I - means the identity matrix.

Other values are selected as: $Q_l = I$ and $R = 0.1I$.

3.1 Case 1: Flight of the formation with a triangular obstacle

In the figure below (Fig. 8) leader (black color), winger number 1 (blue) and wing number 2 (green) are initially aligned along the y axis when the

leader's flight is forced to the target position of 25.0 [m] while maintaining the formation with two wingers, i.e. the ordering separation between them is 1 [m] in the direction of the axis y.

This figure illustrates that the formation is maintained, and the array of UAV objects effectively avoids collision with a triangular obstacle marked in red on the graph.

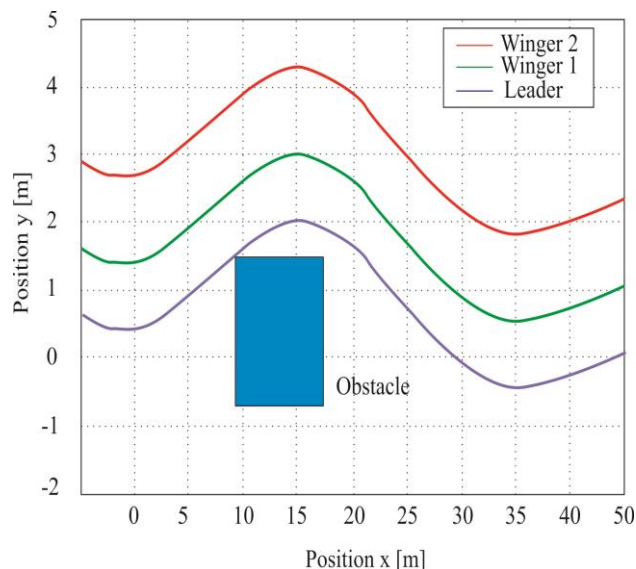


Fig. 8. The scenario of avoiding a collision with an obstacle in the shape of a triangle by the UAV object

3.2 Case 2: Division of formation

The scenario presented in the next figure (Fig. 9) is more complicated than the previous case.

Initially leader (black color), winger number 1 (blue), winger number 2 (green), winger number 3 (turquoise), winger number 4 (pink) are aligned on the y axis with $x = 0$.

Initially the leader is forced to fly to the target position at the height (15.0) [m], and the formation is instructed to maintain the shape of the letter V, as indicated by the red dotted line in the figure below.

Secondly, the 5-vehicle formation is divided into two formation groups, i.e. Group 1 (leader, winger No. 1 and winger No. 2) and Group 2 (winger No. 3 and winger No. 4).

The leader along with the wingman 3 is forced to make a flight towards the target (50.0) [m] and (50.-15) [m] respectively.

This figure illustrates that UAV objects can execute commands while maintaining security.

In addition, if the computing power is sufficient, the better performance by setting the prediction horizon longer can be achieved.

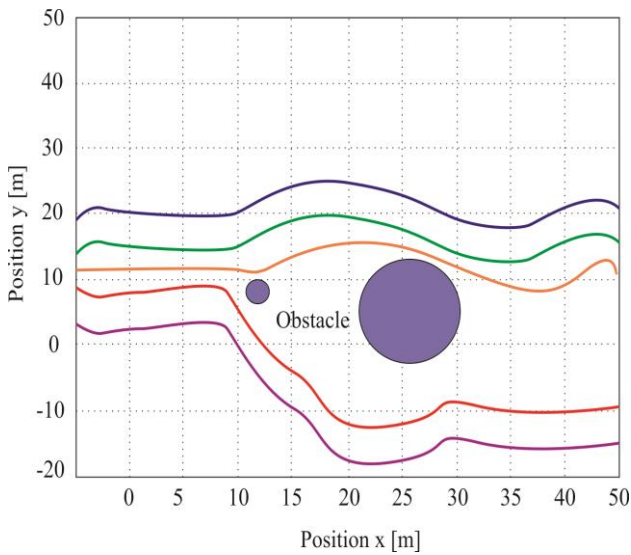


Fig. 9. Division of the formation while avoiding obstacles

3.3 Case 3: Comparison of a robust decentralized approach (with restrictions being defined) with a decentralized approach without a guarantee of resistance

In this simulation, the leader (blue) receives a command to fly to two target points (green circles), and the wing of the UAV object tries to maintain the formation, i.e. 3 [m] from the leader in the y direction.

Both UAV objects are disturbed $\|w_k^i\|_\infty < 1 [m]$, that are randomly entered into the value of position x and y. Flight simulation results of the formation including and without taking into account resistance are illustrated in the following figures (Figures 10 and 11). As expected, without taking into account reliability, a decentralized flight controller loses its feasibility, so it stops when it hits the first obstacle.

At the same time, using a feedback controller and stabilizing the binding, a resistant decentralized flight controller formation can successfully perform the entrusted mission.

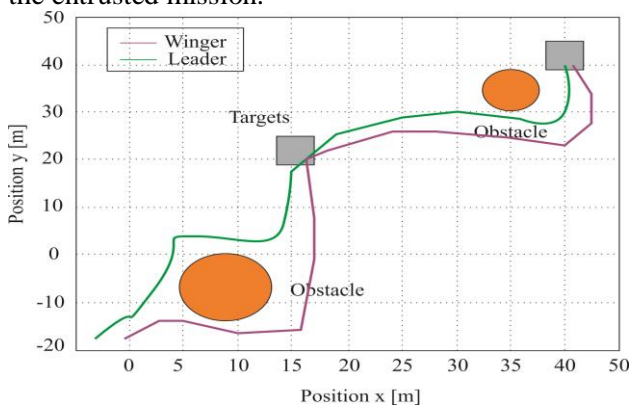


Fig. 10. Decentralized flight of formation

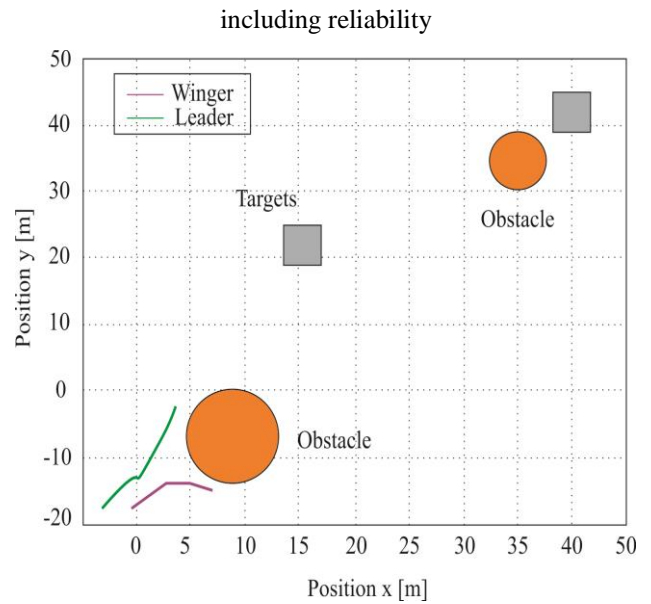


Fig. 11. Decentralized flight of formation without taking into account reliability

3.4 Case 4: Avoiding small obstacles

This simulation shows the benefits resulting from the algorithm to avoid small obstacles. In the figure below (Fig. 12) the expected future point in one step is 1.5 [m], i.e. it is larger than the diagonal of the obstacle, i.e. 1.13 [m], so without imposing a limitation of the position shown in subsection 4.4, the leader "ignores" the obstacle and the flight towards the target position (green circle).

In the next figure (Fig. 13), it can be observed that during the simulation the position limitation was added to the optimization, so in accordance with expectations, formation can effectively avoid a collision with a small obstacle and reach the target position without a collision.

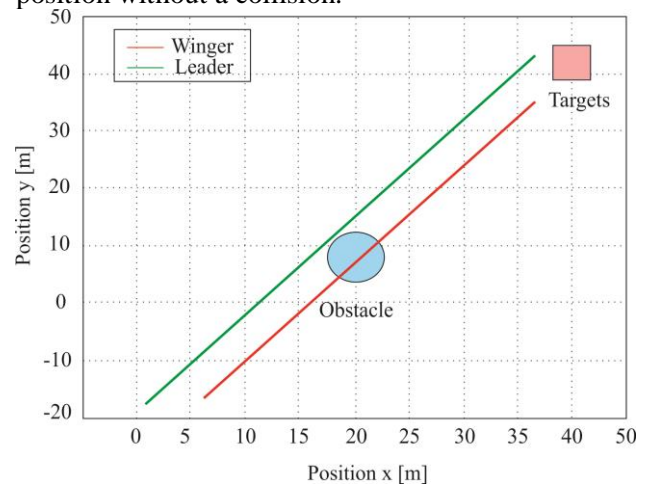


Fig. 12. Flight of the formation without collision with a small obstacle (formation without position restriction)

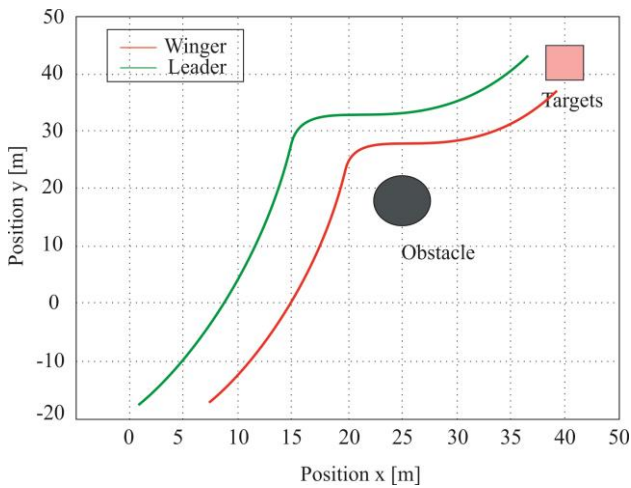


Fig. 13. Flight of the formation without collision with a small obstacle (formation with limited position)

3.5 Case 5: Multiplexed and the nominal decentralized flight control of the formation

This simulation compared the results of multiplexed decentralized flight control of the formation and the nominal decentralized flight control in the formation, which are illustrated in the following figures (Figs. 14-15). Initially, the leader is in position (0, 0), winger number 1 and winger number 2 respectively (0, -3) [m] and (0, -6) [m].

First, the leader is forced to achieve a position equal to target number 1 (green circle) in point (12, 0) [m], but in 1.3 [s] the leader is to make a flight to target number 2 (black circle).

In a multiplexed decentralized diagram, subsystems of UAV objects are updated in sequence (1, 2, 1, 3, 1, 2, 1, 3 ...), which means that the leader will respond faster than the nominal decentralized scheme that updates the subsystem of UAV objects when all input data updates are available. The total simulation time in both cases is 3 [s].

As expected, the formation response illustrated in the figure below (Fig. 15) is faster than in Figure 14. Using a specific update sequence, the operator or ground control station can take full advantage of the advantages of each UAV object subsystem.

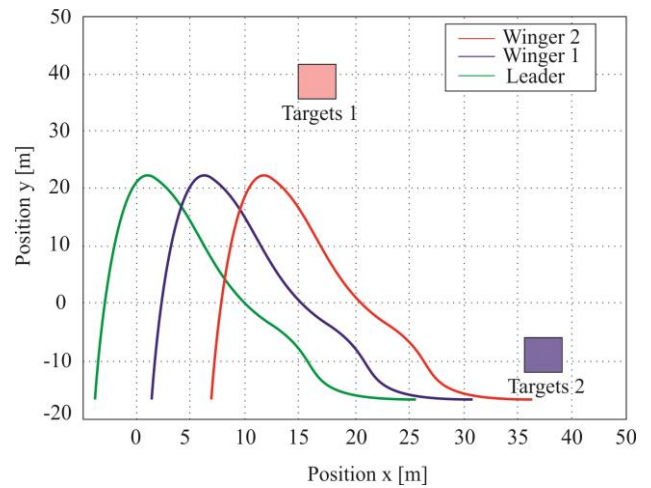


Fig. 14. Multiplexed decentralized formation

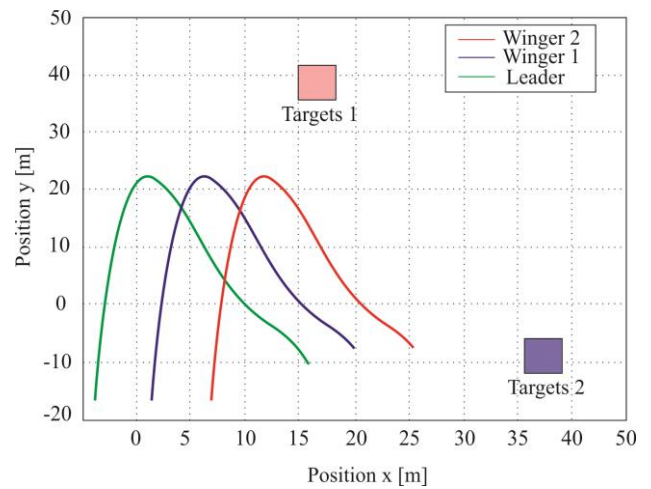


Fig. 15. Nominal decentralized formation

3.6 Case 6: Flight of formation in three-dimensional space (3D)

This simulation serves to show that the schema can be easily expanded in the 3D case, as illustrated in the figure below (Fig. 16).

In the formula of collision avoidance limitation in 3 dimensions, if the UAV object has the ability to hover, several options can be selected, e.g. the UAV object can bypass obstacles on the X-Y, X-Z or Y-Z plane, depending on the current situation or the requirements of the group mission.

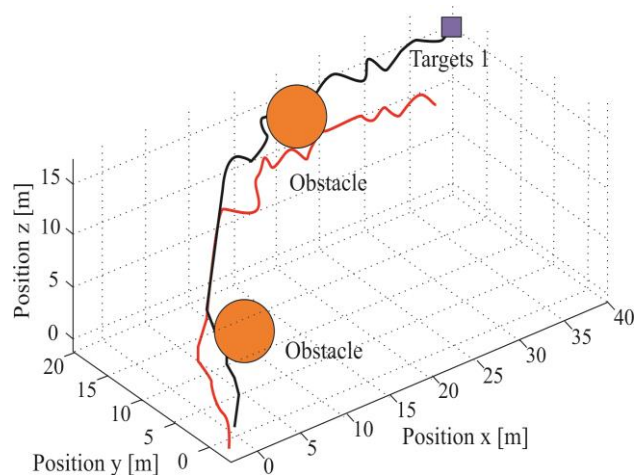


Fig. 16. 3D formation flight

In this subchapter, the controller's approach is used to systematically manage flight control with UAV object formations. When implementing it, the following issues should be carefully considered:

1. If the number of UAV objects in the formation is large, updating one input of the UAV object in each step will be unacceptable because the update interval will be too long. In this case, the update can be applied to a small group of UAV objects each time to reduce the total update interval.
2. In turn, due to the fact that in the controller schedule the update time of each subsystem of the UAV object is fixed, an additional synchronization clock is required in the formation system, which may increase the complexity of the flight system of the formation.

4 Conclusions

The paper presents a developed algorithm for planning an unmanned aerial vehicle route, which takes into account both the constraints imposed by the dynamic properties of this object, as well as other restrictions imposed on the flight route, which were mentioned in this article.

In addition, a method of searching for a quasi-optimal trajectory was proposed in case of a larger number of obstacles. After conducting a series of simulation tests, it can be concluded that the time of route determination using the developed algorithm depends on several factors.

The first attribute is the area of terrain discretization (grid size). The smaller the mesh, the more accurately the terrain can be mapped, but the calculation time increases, because there will be more vertices to check.

Another factor that significantly more affects the calculation time is the complexity of the area in which the flying object will fly.

The more obstacles (terrain_shape and prohibited zones) are in this area and the more restrictions are placed on the route, the calculation time is greater, because the algorithm must find an alternative route taking into account the mentioned limitations and the capabilities of the flying object.

Although the developed algorithm is not computationally complex, one could think about the method of grouping obstacles to speed up the operation of this algorithm.

However, this is a separate issue that can be the subject of further research.

References:

- [1] Singh S.N., Zhang R., Chandler P., Banda S., "Decentralized nonlinear robust control of UAVs in close formation," *International Journal of Robust and Nonlinear Control*, 2003.
- [2] Setlak L., Kowalik R., "Algorithm Controlling the Autonomous Flight of an Unmanned Aerial Vehicle based on the Construction of a Glider," *WSEAS Transactions on Applied and Theoretical Mechanics*, Volume 14, pp. 56-65, 2019.
- [3] Richards A., How J., "Decentralized model predictive control of cooperating UAVs," *IEEE Conference on Decision and Control*, Atlantis, 2004.
- [4] Zelinski S., Koo T.J., Sastry S., "Hybrid system design for formations of autonomous vehicles," *Conference on Decision and Control*, California, 2003.
- [5] Keck-Voon L., MACIEJOWSKI J., Bing-Fang W., "Multiplexed Model Predictive Control," *16th IFAC World Congress*, Prague, 2005.
- [6] Setlak L., Kowalik R., "Stability Evaluation of the Flight Trajectory of Unmanned Aerial Vehicle in the Presence of Strong Wind," *WSEAS Transactions on Systems and Control*, Volume 14, pp. 43-50, 2019.
- [7] Chena J., Sun D., Yang J., Chen H., "A leader-follower formation control of multiple nonholonomic mobile robots incorporating receding-horizon scheme," *The International Journal of Robotics Research*, 2009.
- [8] Gu Y., Seanor B., Campa G., Napolitano M.R., Rowe L., Gururajan S., Wan S., "Design and flight testing evaluation of formation control laws," *Control Systems Technology*, IEEE Transactions, 2006.

- [9] Pachter M., D'azzo J., Dargan J., "Automatic formation flight control," *Journal of Guidance, Control, and Dynamics*, 1994.
- [10] Schumacher, C. and R. Kumar, "Adaptive control of UAVs in close-coupled formation flight," *American Control Conference*, Chicago, 2000.
- [11] Ayanian N., Kumar V., "Decentralized Feedback Controllers for Multiagent Teams in Environments With Obstacles," *Robotics, IEEE Transactions*, 2010.
- [12] Setlak L., Kowalik R., "Dynamics of the Designed Robotic Manipulator in the CAD Program," *WSEAS Transactions on Applied and Theoretical Mechanics*, Volume 14, pp. 66-74, 2019.
- [13] Borrelli F., Subramanian D., Raghunathan A.U., Biegler L.T., "MILP and NLP Techniques for centralized trajectory planning of multiple unmanned air vehicles," *American Control Conference*, Minneapolis, 2006.
- [14] Ousingsawat J., Campbell M., "Establishing trajectories for multi-vehicle reconnaissance," 2004.
- [15] Singh S.N., Chandler P., Schumacher C., Banda S., Pachter M., "Adaptive feedback linearizing nonlinear close formation control of UAVs," *American Control Conference*, Chicago, 2000.
- [16] Pachter M., D'Azzo J., Proud A., "Tight formation flight control. *Journal of Guidance, Control, and Dynamics*," 2001.
- [17] Kim Y., Tahk M.J., Jeon G.E., "Cascade-type guidance law design for multiple - UAV formation keeping," *Aerospace Science and Technology*, 2010.
- [18] Jie M., Wei R., Guangfu M., "Distributed Coordinated Tracking With a Dynamic Leader for Multiple Euler-Lagrange Systems," *Automatic Control, IEEE Transactions*, 2011.
- [19] Freitas E.P., Heimfarth T., Ferreira A.M., Pereira C.E., Wagner F.R., Larsson T., "Decentralized Task Distribution among Cooperative UAVs in Surveillance Systems Applications," *Seventh International Conference on Wireless On-demand Network Systems and Services*, Piscataway, 2010.
- [20] Guerrero J.A., Romero G., Lozano R., "Robust consensus tracking of leader-based multi-agent systems," *American Control Conference (ACC)*, Baltimore, 2010.
- [21] Setlak L., Kowalik R., Bodzon S., "The Study of Air Flows for an Electric Motor with a Nozzle for an Unmanned Flying Platform," *WSEAS Transactions on Fluid Mechanics*, Volume 14, pp. 21-35, 2019.